JOURNAL OF MATERIALS SCIENCE **36** (2001) 4307–4313

Morphology of solution-grown poly(β-propiolactone) single crystals

Y. FURUHASHI, T. IWATA, Y. DOI*
Polymer Chemistry Laboratory and the RIKEN Group of Japan Science and Technology Corporation, RIKEN Institute, Hirosawa, Wako-shi, Saitama 351-0198, Japan
E-mail: ydoi@postman.riken.go.jp

Single crystals of poly(β-propiolactone) (PPL) with different molecular weights ($M_w = 70\,000$ and $M_w = 2300$) were grown from four kinds of solvents under isothermal crystallization condition. The morphologies and crystal structures of PPL single crystals were investigated by means of transmission electron microscopy and atomic force microscopy. The single crystals of high-molecular-weight PPL (HMW-PPL) grown from cyclohexanone appeared elongated with dimensions of around 0.2–0.8 μm along the short and 5–10 μm along the long axes. Single crystals of low-molecular-weight PPL grown from cyclohexanone showed three to five elliptical-shaped lamellae, from central nucleus like petals. The long axes of both single crystals corresponded to the crystallographic *b* axis. The reciprocal lattice parameters: $a^* = 2.045$ nm^{-1}, $b^* = 1.420$ nm^{-1} and $\gamma^* = 90^\circ$ could be determined from electron diffractograms. Decoration of the crystals with polyethylene suqqested that the single crystals of HMW-PPL have regular chain-folding along their long axis in the [010] direction with consecutive folds in the [110] and [1$\bar{1}$0] directions. Accordingly, it is deduced that HMW-PPL has the anti-parallel chain-packing structure.

1. Introduction

Poly (β-propiolactone) (PPL) is a biodegradable thermoplastic. Yamashita *et al*. have reported that PPL films obtained by extrusion molding and drawing processes exhibited high tensile strengths and elongations to breaking and high moisture permeabilityies [1]. Moreover, Tasaka *et al*. have reported recently that ferroelectric behavior due to the C=O dipole rotation was observed in semicrystalline PPL [2].

Ring-opening polymerization of β-propiolactone, a four-membered lactone, has been widely studied mainly by chemical synthesis using acids, bases and salts as catalysts [3–7]. Also PPL has been prepared by radiation-induced polymerization at low temperature [8–11]. Furthermore, it is well known that β-propiolactone can be polymerized by anions [12–19] or cation [20] and by alkali metals [21] or metal alkoxide [22]. Recently, in addition to these chemical syntheses, enzyme-catalyzed ring-opening polymerization has also been studied [23–25].

Although PPL is a chemosynthetic polymer, PPL is biodegraded by enzymes or microorganisms in natural environments. Asano *et al*. have studied the degradation of melt-pressed PPL by implanting it into the back of rats [26, 27]. They reported that *in vivo* degradation of the polymer was strongly dependent upon the crystallinity. Nishida *et al*. have reported the distribution of PPL aerobic degrading microorganisms in different environments [28]. Seventy-seven strains of PPL degrading microorganisms were isolated, and at least 41 strains were referred to as *Bacillus* species. Concerning enzymatic degradation, it is known that PPL is degraded by both polyhydroxyalkanoates (PHA) depolymerases and lipases. Tokiwa and Suzuki have reported that PPL is hydrolyzed by *Rhizopus delemar* lipase [29]. Baba *et al*. have reported that PPL is degraded by an extracellular PHA depolymerase from *Alcaligenes faecalis* T1 [30].

The crystal structure of PPL has been widely investigated by infrared adsorption and X-ray diffraction [4, 5, 7, 8, 10, 11, 31, 32]. X-ray studies showed that PPL has two crystalline modifications depending on drawing and annealing conditions [31, 32]. These modifications are defined as the α and β forms, representing 2_1 helix (fiber repeat 0.702 nm [31]) and planar-zigzag (fiber repeat 0.482 nm [31], 0.477 nm [32]) conformations, respectively. The β form showed a unique X-ray fiber pattern, i.e., discrete reflections on the equatorial line and diffuse continuous scattering on the layer lines. It was found that the X-ray fiber pattern of the β form indicated a disordered packing of the molecular chains in the crystal lattice with random displacement along the fiber axis. On the other hand, Asahara and Katayama have reported that PPL

*Author to whom all correspondence should be addressed.

has three crystal structures, which are helical, 2_1 helix and zigzag structures, depending on the polymerization method [7].

Although many researchers have investigated the crystal structures and conformations of PPL, no detail analysis has been reported. Preparing single crystals that have clear, uniform and well-defined structure is useful for elucidating the crystal structure. In this paper, the first preparation of single crystals of PPL grown from a variety of solvents is reported. Also, the morphology and chain-folding structure of PPL single crystals is investigated by means of transmission electron microscopy and atomic force microscopy.

2. Experimental

2.1. PPL samples

PPL sample (weight-average molecular weight (M_w) = 367 000 and polydispersity (DPI) = 2.2) was supplied by Tokuyama Corporation. The PPL sample was purified by precipitation in methanol from chloroform solution and dried in an oven at 35°C. Two different molecular weight PPLs (high-molecular-weight (HMW-PPL), $M_w = 70\,000$ and DPI = 1.6, and low-molecular-weight PPL (LMW-PPL), $M_w = 2\,300$ and DPI = 1.5) were prepared by using 1 N aqueous KOH alkali-hydrolysis with 18-crown-6 ether, according to the method reported previously [33]. Purified PPL (50 mg) was dissolved in chloroform (6 ml). After adding 40 mg of 18-crown-6 ether to the PPL solution, the mixture was kept at 35°C and stirred for 2.5 h or 6 h. The organic layer was pipetted into a sample vessel and dried over anhydrous magnesium sulfate. After filtering, the organic layer was precipitated into methanol.

2.2. Preparation of single crystals

Single crystals were prepared from a dilute solution under isothermal crystallization conditions. The solvents used for solution-grown single crystals were cyclohexanone, α-chloronaphthalene, *o*-dichlorobenzene and 1, 4-butanediol, all of which were normal laboratory grade chemicals. One mg of PPL was dissolved in 4 ml of solvent at high temperature, which was maintained for 1 h in a silicone oil bath. Crystals obtained by dissolution and slow cooling are complex aggregates. Accordingly, attempts were made to improve the crystals grown from solution by using isothermal crystallization conditions. These are summarized in Table I.

2.3. Transmission electron microscopy

To collect the single crystals, centrifugation and washing the crystals with methanol at room temperature were used, except for crystals grown from cyclohexanone. A drop of methanol containing single crystals was deposited on a carbon-coated grid and allowed to dry, and then shadowed with a Pt-Pd alloy. For diffraction studies, the crystals were allowed to dry and were not coated. In the case of cyclohexanone solution, when methanol was added to the crystal suspension for washing, the single crystals aggregated. The same observations were obtained for ethanol and acetone. Furthermore, centrifugation caused the single crystals to be broken into pieces. Thus, a drop of PPL single crystals in cyclohexanone solution was directly deposited on a carbon-coated grid, and allowed to dry completely. The decoration of crystals with polyethylene was performed by evaporating polyethylene on the crystals under vacuum, according to the method of Wittman and Lotz [34].

A JEM-2000FX II transmission electron microscope operated at an acceleration voltage of 120 kV was used. The observations were mostly performed at room temperature; sometimes the specimens were kept at liquid nitrogen temperature by using a cryo-holder. For calibration purposes, some crystals were mounted on carbon-coated grids sputtered with gold. All calibration was performed at room temperature.

2.4. Atomic force microscopy

The thicknesses of PPL single crystals were measured using atomic force microscopy (AFM). A drop of crystal suspension was placed on mica and allowed to dry. AFM was performed with a SPI3700/SPA300 (Seiko Instruments Inc.). Pyramid-like Si_3N_4 tips, mounted on 100 μm long microcantilevers with spring constants of 0.09 N/m, were applied for the contact mode experiments. Simultaneous registrations were performed in the contact mode for height and deflection images. All images were recorded at room temperature.

3. Results and discussion

3.1. Morphology of single crystals grown from different solvents

Fig. 1 shows HMW-PPL single crystals grown from four kinds of solvents. In all the preparations the crystals aggregated. Crystals grown from all solvents, except for 1, 4-butanediol, were lath-shaped. Single crystals grown from cyclohexanone, as shown in Fig. 1a, yielded lath-shaped lamellae dimensions of around 0.5–1.5 μm along the short and of around 5–8 μm along the long axes. This morphology resembles that of single crystals of poly([*R*]-3-hydroxybutyrate) (P(3HB)) [33, 35–38]. The crystals grown from α-chloronaphthalene were lath-shaped lamellae which had the dimensions of around 0.2–0.8 μm along the short and of around 5–10 μm along the long axes

TABLE I Details of the dissolution and crystallization conditions for solution-grown single crystals of poly(β-propiolactone)

Solvent	Concentration (%, (wt/vol))	Dissolution temperature (°C)	Cloudy temperature (°C)	Crystallization temperature (°C)	Crystallization time (h)
Cyclohexanone	0.025	70	35	55	36
α-Chloronaphthalene	0.025	185	110	100	76
o-Dichlorobenzene	0.025	160	80	80	6
1,4-Butanediol	0.025	90	70	70	6

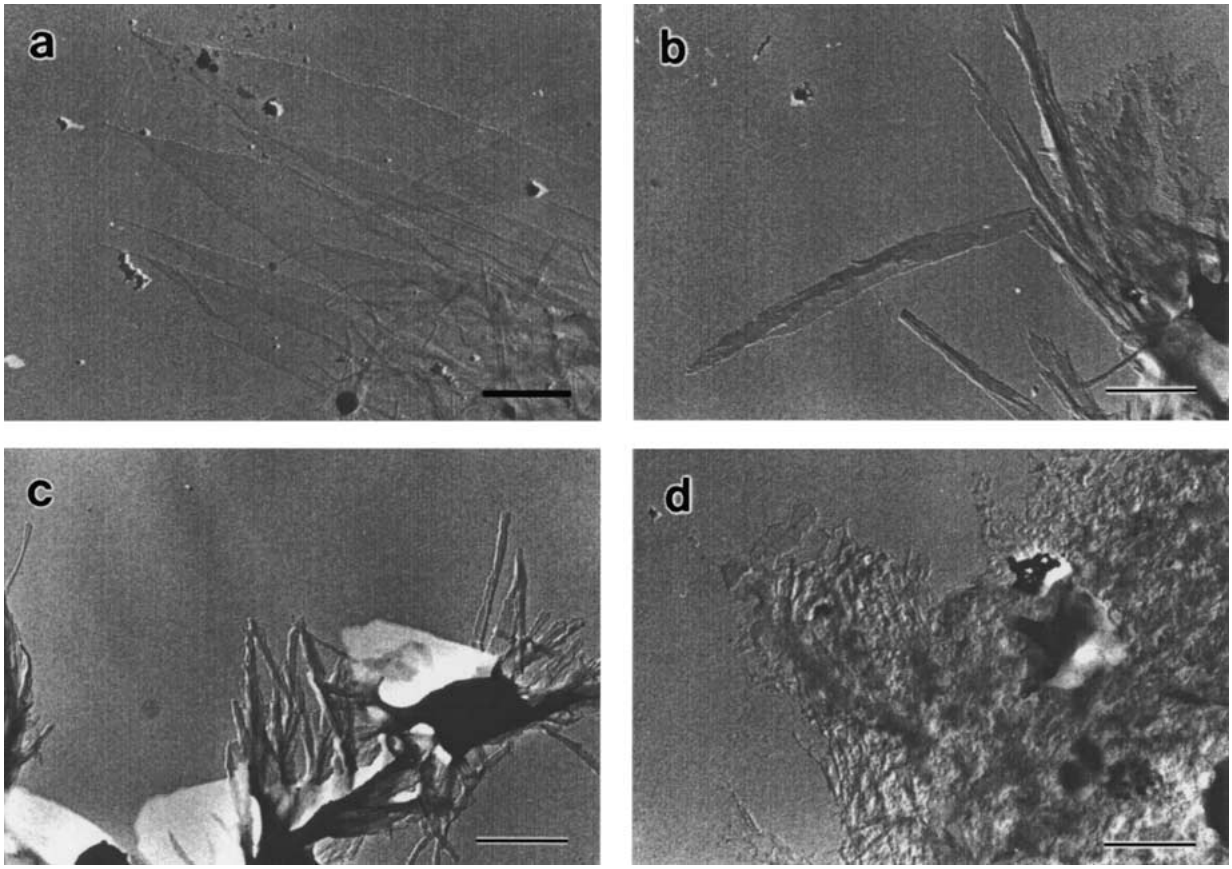

Figure 1 Electron micrographs of HMW-PPL single crystals grown from dilute solution in (a) cyclohexanone, (b) α-chloronaphthalene, (c) *o*-dichlorobenzene and (d) 1,4-butanediol. Scale bars represent 1 μm.

(Fig. 1b). The crystals grown from *o*-dichlorobenzene showed both very thick and narrow needle-like lamellae (Fig. 1c). In the case of 1, 4-butanediol solution, very small particles in aggregated stacks were observed. (Fig. 1d).

The single crystals of HMW-PPL grown from cyclohexanone solution showed the best morphology for further investigation within solvents used in this study. Accordingly, LMW-PPL single crystals were prepared using cyclohexanone. In the case of HMW-PPL grown from cyclohexanone solution, the cloudy temperature was 35°C on slow cooling to room temperature. In the case of LMW-PPL in cyclohexanone solution, no cloudy temperature was obtained and no single crystals were observed at room temperature. However, when the solution was kept in a refrigerator (4°C), single crystals were observed. Consequently, the cloudy temperature of LMW-PPL is lower than room temperature.

LMW-PPL single crystals showed two types of morphology, as shown in Fig. 2. One form comprised three to five elliptical-shaped lamellae joined to a central nucleus like petals, as shown in Fig. 2a. The size of the lamellae was around 0.7–1.5 μm along the short and around 2–5 μm along the long axes. This morphology of LMW-PPL single crystals resembles two-dimensional spherulites in polyethylene [39], although the spherulites are bigger. The other morphology, as shown in Fig. 2b, showed short lath-shaped lamellae, with jagged edges. Moreover, striations running parallel to the long axis of single crystals could be observed on the crystal surfaces. This striation phenomenon is discussed later.

3.2. Electron diffraction study

Selected-area electron diffraction was performed for both HMW- and LMW-PPL single crystals grown from a dilute solution of cyclohexanone. The HMW-PPL single crystals produced a spot diffraction pattern, with a minimum spacing of 0.135 nm. In the case of LMW-PPL single crystals, the elliptical-shaped lamellae (Fig. 2a) yielded well-resolved electron diffraction with a spacing of 0.115 nm, while that of the lath-shaped monolamellae (Fig. 2b) showed **ark** diffraction.

To determine the orientation of the crystal axis, triple-exposure experiments on the HMW- and LMW-PPL single crystals were performed. Fig. 3 shows an electron diffraction pattern from an elliptical-shaped LMW-PPL single crystal. The crystallographic *b* axis lies along the long axis of the crystal and the sides do not correspond to any low index plane. The diagram contains 21 independent diffraction spots mirrored in the four quadrants defined by the two orthogonal axes a^* and b^*. Upon calibration of the electron diffraction pattern, all the electron diffraction spots can be indexed in terms of orthogonal reciprocal lattice parameters: $a^* = 2.045$ nm^{-1}, $b^* = 1.420$ nm^{-1} and $\gamma^* = 90°$.

3.3. Chain-folding structure

Fig. 4 shows AFM images and line profile data of HMW- and LMW-PPL single crystals. The thicknesses by AFM of the monolamellar part of both single crystals yielded values of around 5 nm, in spite of the difference in molecular weight. Based on the lamellar thickness and the molecular weight of the polymer,

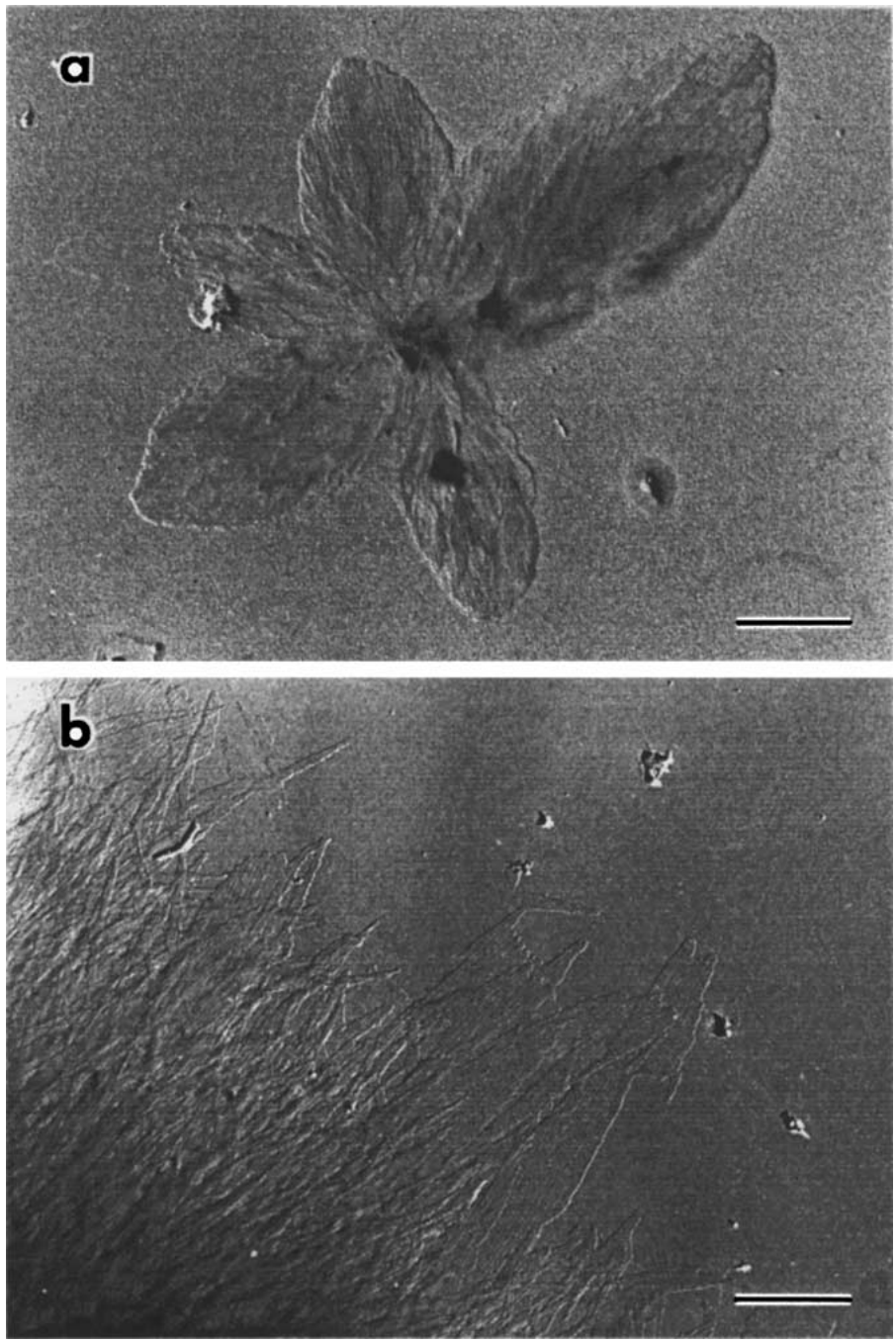

Figure 2 Electron micrographs of LMW-PPL single crystals grown from solution in cyclohexanone, (a) elliptical-shaped and (b) lath-shaped. Scale bars represent 1 μm.

it is suggested that the molecular chains of HMW-PPL are folded within the lamella. In the case of LMW-PPL, taking the degree of polymerization of PPL and the fiber repeat distance along the molecular axis of either α form or β form [31, 32] into consideration, chain-folding at the lamellar surface may not occur.

The polymer decoration method developed by Wittman and Lotz [34], has been widely used to study the chain-folding behavior of polymer crystals, such as polyethylene [34, 40, 41], poly(ethylene oxide) [42], P(3HB) [36] and odd polyoxamide [43]. Crystallization of polyethylene on the surface of the crystal is a useful technique to reveal the chain-folding surface structure. It was found that the direction of the long axis of the polyethylene crystals is perpendicular to the direction of chain-folding on single crystals.

Fig. 5 shows single crystals of HMW-PPL decorated with polyethylene and shadowed with a Pt-Pd alloy. Decoration of HMW-PPL single crystals shows rods of crystallized polyethylene, and they were relatively ordered perpendicular to the long axis of the single crystals. Accordingly, molecular chain-folding on PPL single crystals should be occurring along the long axis of the single crystals; i.e. the *b* axis of crystals. When molecular chains fold, there should have alternate crystalline **stems** "up" and "down" in the lattice, i.e. anti-parallel. Therefore, chain-packing of HMW-PPL single crystals occurs anti-parallel with intramolecular interaction. No sectorization is observed in the polyethylene decorated HMW-PPL crystal. Consequently, the chain-folding direction is constant in all parts of the crystal. LMW-PPL however has no

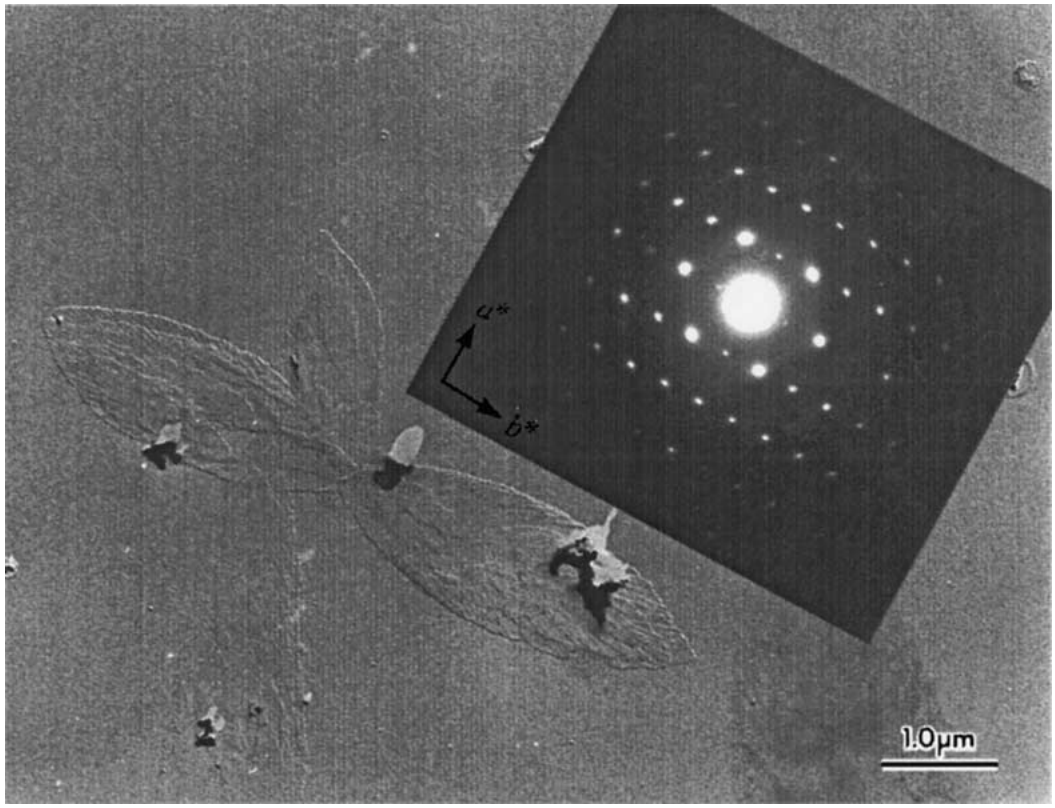

Figure 3 Typical electron diffractogram corresponding to an LMW-PPL single crystal.

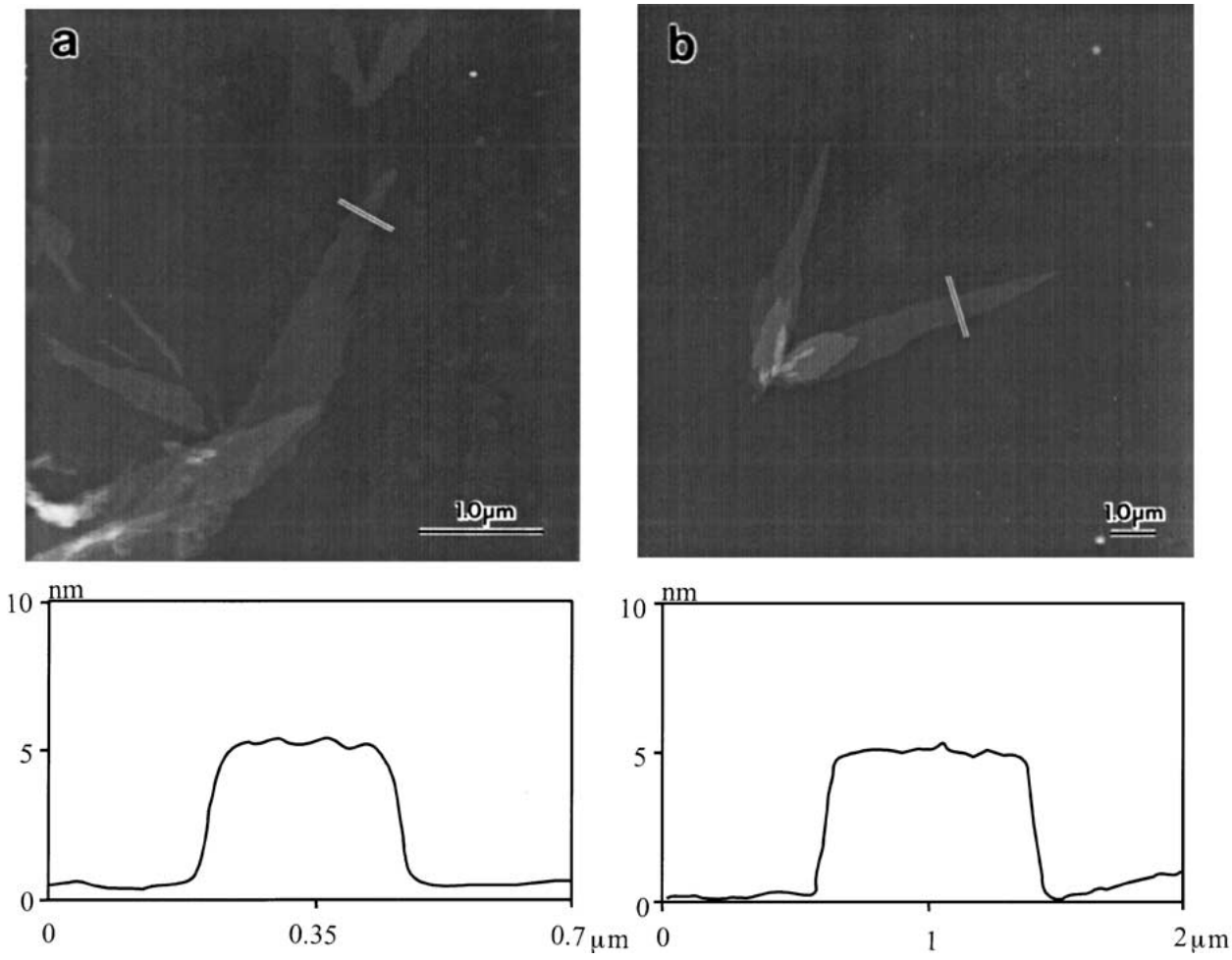

Figure 4 AFM images and line profile data of (a) HMW-PPL and (b) LMW-PPL.

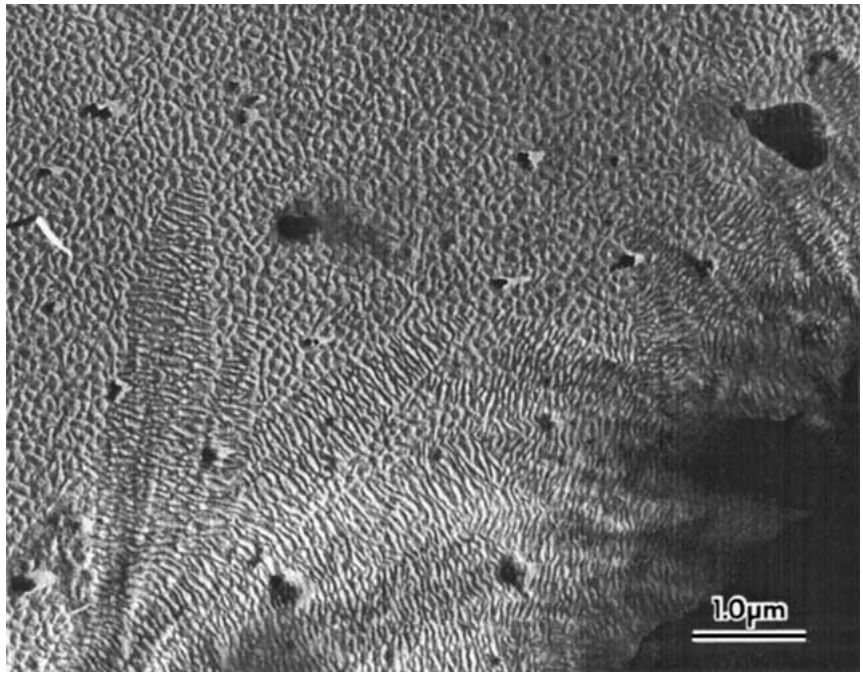

Figure 5 Electron micrograph of HMW-PPL single crystals decorated with polyethylene and shadowed with a Pt-Pd alloy.

appearance of rods (data not shown), suggesting that no polyethylene is decorated on the crystal surface. Therefore, LMW-PPL single crystals have no regular chain-folding.

In the case of P(3HB), Birley *et al*. reported a folded-surface structure [36]. They suggested that the overall direction of folding is along the [100] direction, and that the chains which fold in the [110] direction at one surface of the crystal fold back at the opposite surface along the $[1\bar{1}0]$ direction. In this study, the HMW-PPL folding occurs along the [010] direction. However, the close-packed plane along which regular folding is possible is the {110} plane. Having deduced that the chain-folding in HMW-PPL crystals should be quite regular with a high degree of adjacency, a possible adjacent fold for a chain emerging from a HMW-PPL crystal is along one of the ⟨110⟩. Because the overall direction of folding is along the [010] direction, it is deduced that the chains that fold in the [110] direction at one surface of the crystal fold back at the opposite surface along the $[1\bar{1}0]$ direction, as illustrated in Fig. 6.

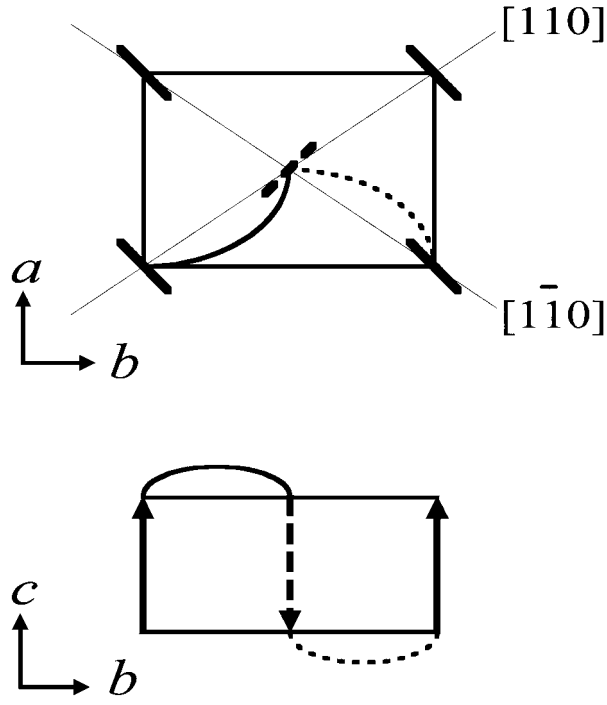

Figure 6 Projection of PPL structure in the *ab* and *bc* planes. Molecular backbone are shown as (\) and (/) for "up" chain (↑) and "down" chain (↓), respectively. Fold on upper fold surface (⌒) and fold on lower surface (⌣) are shown.

3.4. Morphology of LMW-PPL single crystals with striations

LMW-PPL single crystals showed two morphologies. Both crystal surfaces were decorated with striations running parallel to the long axis of the crystal with a regular spacing of about 30 nm. This morphology is also observed in some HMW-PPL single crystals Buléon *et al*. have reported that single crystals of cellulose II have ribbon or needle-like lamella with a growth plane of (110) [44]. Surface striations are also observed, running at an angle of 65° to the axis of the ribbon, and along (020) planes of the cellulose II lattice.

In the case of LMW-PPL, the crystal surface is decorated with striations running parallel to the long axis corresponding to the crystallographic *b* axis at regular intervals. The striation phenomenon can be explained in three ways. Firstly, the striations may occur by shifts along the chain axis of molecular chains. The β form of PPL consists of a disordered packing of the molecular chains in the crystal lattice with random displacement along the fiber axis [31, 32]. Secondly, the striations might result from molecular chains being inclined to the basal plane at a constant interval with adjacent molecular chains inclined in the opposite direction. As a consequence, phase-contrast is observed in the micrograph. Thirdly, the striations might be the result of overgrowth or epitaxial growth on the lamellae. Since

the striations occur at constant intervals, the overgrowth or epitaxially growth must occur regularly.

4. Conclusions

Single crystals of poly(β-propiolactone) (PPL) with different molecular weights were prepared in a cyclohexanone solution under isothermal crystallization conditions. The single crystals of high-molecular-weight PPL (HMW-PPL, $M_w = 70\,000$) formed lath-shaped lamellae. Low-molecular-weight PPL (LMW-PPL, $M_w = 2\,300$) crystals showed two morphologies; one with elliptical-shaped lamellae attached to a central nucleus like petals, and the other with lath-shaped lamellae. The reciprocal lattice parameters: $a^* = 2.045\,\mathrm{nm}^{-1}$, $b^* = 1.420\,\mathrm{nm}^{-1}$ and $\gamma^* = 90^\circ$ could be determined from electron diffractograms. The crystallographic b axes of HMW- and LMW-PPL single crystals corresponded to the long axes of the crystals. By using polyethylene decoration, the orientation of polyethylene rods were found to lie perpendicular to the long axis of HMW-PPL single crystals. Consequently, it was revealed that the average direction of molecular chain-folding occurs along the [010] direction suggesting that consecutive folds occur in the [110] and [1$\bar{1}$0] directions and that the single crystals of HMW-PPL crystallize with intramolecular interaction with anti-parallel chain-packing.

Acknowledgements

The authors wish to thank Dr. H. Nishida of Tsukuba Research Laboratory, Tokuyama Corporation for providing the samples used in this study. We are also grateful to Dr. J. Sugiyama of Wood Research Institute, Kyoto University for a stimulate discussion regarding the morphology of striation. This work has been supported by CREST (Core Research for Evolutional Science and Technology) of Japan Science and Technology Corporation (JST), a grant of Ecomolecular Science Research provided to RIKEN Institute by the Science and Technology Agency (STA) of Japan, and a grant-in-aid for Scientific research on Priority Area, "Sustainable Biodegradable Plastics" from the Ministry of Education, Science, Sports and Culture, Japan (No. 11217216).

References

1. M. YAMASHITA, N. HATTORI and H. NISHIDA, *Polymer Preprints, Japan* **43** (1994) 3979.
2. S. TASAKA, M. KAWAGUCHI and N. INAGAKI, *Eur. Polym. J.* **34** (1998) 1743.
3. T. L. GRESHAM, J. E. JANSEN and F. W. SHAVER, *J. Amer. Chem. Soc.* **70** (1948) 998.
4. S. OKAMURA, T. HIGASHIMURA and A. TANAKA, *J. Chem. Soc. Japan, Ind. Chem. Sect.* **65** (1962) 707.
5. S. OKAMURA, T. HIGASHIMURA, A. TANAKA, R. KATO and Y. KIKUCHI, *Makromol. Chem.* **54** (1962) 226.
6. S. ASAHARA and S. KATAYAMA, *J. Chem. Soc. Japan, Ind. Chem. Sect.* **69** (1966) 725.
7. S. ASAHARA and S. KATAYAMA, *ibid.* **69** (1966) 2179.
8. S. OKAMURA, K. HAYASHI, Y. KITANISHI and M. NISHII, *Isotopes and Radiation* **3** (1960) 510.
9. K. HAYASHI and S. OKAMURA, *Makromol. Chem.* **47** (1961) 230.
10. K. HAYASHI, Y. KITANISHI, M. NISHII and S. OKAMURA, *ibid.* **47** (1961) 237.
11. S. OKAMURA, K. HAYASHI and Y. KITANISHI, *J. Polym. Sci.* **58** (1962) 925.
12. Y. YAMASHITA, K. ITO and F. NAKAKITA, *Makromol. Chem.* **127** (1969) 292.
13. V. JAACKS and N. MATHES, *ibid.* **131** (1970) 295.
14. S. SLOMKOWSKI and S. PENCZEK, *Macromolecules* **9** (1976) 367.
15. *Idem., ibid.* **13** (1980) 229.
16. A. HOFMAN, S. SLOMKOWSKI and S. PENCZEK, *Makromol. Chem.* **185** (1984) 91.
17. S. SOSNOWSKI, S. SLOMKOWSKI, S. PENCZEK, G. N. ARKHIPOVICH and K. S. KAZANSKII, *ibid.* **188** (1987) 1347.
18. Z. JEDLINSKI, M. KOWALCZUK and P. KURCOK, *Macromolecules* **24** (1991) 1218.
19. H. R. KRICHELDORF, N. SCHARNAGL and Z. JEDLINSKI, *Polymer* **37** (1996) 1405.
20. J. M. JONTE, R. DUNSING and H. R. KRICHELDORF, *J. Macromol. Sci. Chem.* **A23** (1986) 495.
21. Z. JEDLINSKI, P. KURCOK and M. KOWALCZUK, *Macromolecules* **18** (1985) 2679.
22. H. R. KRICHELDORF, M. BERL and N. SCHARNAGL, *ibid.* **21** (1988) 286.
23. S. MATSUMURA, H. BEPPU, K. TSUKADA and K. TOSHIMA, *Biotechnol. Lett.* **18** (1996) 1041.
24. G. A. R. NOBES, R. J. KAZLAUSKAS and R. H. MARCHESSAULT, *Macromolecules* **29** (1996) 4829.
25. S. NAMEKAWA, H. UYAMA and S. KOBAYASHI, *Polym. J.* **28** (1996) 730.
26. M. ASANO, M. YOSHIDA, I. KAETSU, Y. MORITA, H. FUKUZAKI, T. MASHIMO, H. YUASA, K. IMAI, H. YAMANAKA, U. KAWAHARADA and K. SUZUKI, *Kobunshi Ronbunshu* **44** (1987) 897.
27. M. ASANO, M. YOSHIDA, H. FUKUZAKI, M. KUMAKURA, T. MASHIMO, H. YUASA, K. IMAI and H. YAMANAKA, *Eur. Polym. J.* **26** (1990) 29.
28. H. NISHIDA, S. SUZUKI and Y. TOKIWA, *J. Environ. Polym. Degrad.* **6** (1998) 43.
29. Y. TOKIWA and T. SUZUKI, *Nature* **270** (1977) 76.
30. H. BABA, N. TANAHASHI, Y. KUMAGAI and Y. DOI, *J. Chem. Soc. Japan* **5** (1992) 527.
31. T. WASAI, T. SAEGUSA and J. FURUKAWA, *J. Chem. Soc. Japan, Ind. Chem. Sect.* **67** (1964) 601.
32. K. SUEHIRO, Y. CHATANI and H. TADOKORO, *Polym. J.* **7** (1975) 352.
33. T. IWATA, Y. DOI, K. KASUYA and Y. INOUE, *Macromolecules* **30** (1997) 833.
34. J. C. WITTMAN and B. LOTZ, *J. Polym. Sci. Polym. Phys. Ed.* **23** (1985) 205.
35. R. H. MARCHESSAULT, S. COULOMBE, H. MORIKAWA, K. OKAMURA and J. F. REVOL, *Can. J. Chem.* **59** (1981) 38.
36. C. BIRLEY, J. BRIDDON, K. E. SYKES, P. A. BARKER, S. J. ORGAN and P. J. BARHAM, *J. Mater. Sci.* **30** (1995) 633.
37. G. A. R. NOBES, R. H. MARCHESSAULT, H. CHANZY, B. H. BRIESE and D. JENDROSSEK, *Macromolecules* **29** (1996) 8330.
38. T. IWATA, Y. DOI, T. TANAKA, T. AKEHATA, M. SHIROMO and S. TERAMACHI, *ibid.* **30** (1997) 5290.
39. T. KAWAI and A. KELLER, *Phil. Mag.* **11** (1965) 1165.
40. J. J. POINT, *Polymer* **33** (1992) 2469.
41. A. KAWAGUCHI, M. OHARA and M. TSUJI, *J. Polym. Sci: Part B: Polym. Phys.* **32** (1994) 421.
42. J. CHEN, S. Z. D. CHENG, S. S. WU, B. LOTZ and J. C. WITTMANN, *ibid.* **33** (1995) 1851.
43. L. FRANCO, J. A. SUBIRANA and J. PUIGGALI, *Macromolecules* **31** (1998) 3912.
44. A. BULEON and H. CHANZY *J. Polym. Sci., Polym. Phys. Ed.* **16** (1978) 833.

Received 3 November 1999
and accepted 30 March 2001